Advances in Aircraft and Spacecraft Science, *Vol. 13, No. 1 (2026) 45-65*
https://doi.org/10.12989/aas.2026.13.1.045

Techno-Press

Disturbance-observer-augmented Backstepping control for sea-skimming UAVs under severe wave uncertainties

Yunpeng Ji*, Maria S. Selezneva[a]

Faculty of automatic systems, Bauman Moscow State Technical University, Moscow, 2nd Baumanskaya str., 5, p. 1, Russia

(Received February 13, 2025, Revised January 8, 2026, Accepted January 10, 2026)

Abstract. A sea-skimming unmanned aerial vehicle (UAV) is a specialized type of aircraft capable of performing tasks at low altitudes above sea level. However, under extreme sea conditions, wave disturbances introduce significant errors in measuring the relative distance between the UAV and the sea surface, which complicates the control system and degrades flight performance. While existing research primarily relies on filtering or adaptive control methods, their effectiveness in handling non-Gaussian disturbances remains limited. In this paper, a mathematical model for the altitude and pitch motion of a sea-skimming UAV is established, taking into account external disturbances caused by sea wave height. A control method integrating Backstepping theory with a nonlinear disturbance observer (NDO) is designed to ensure system stability. The key innovation of this work lies in using the NDO to estimate and compensate for aggregated disturbances, thereby enabling the Backstepping controller to achieve exponential stability without a parameter adaptation process. Furthermore, a quasi-adaptive coefficient function is incorporated into the NDO to adjust its gains in real time, improving estimation performance. The stability of the proposed method is rigorously proven using Lyapunov theory. Simulation results demonstrate the effectiveness of the NDO-based Backstepping control scheme, showing that it maintains a tracking accuracy of 98.52% even under severe level 7 sea condition.

Keywords: backstepping control; lyapunov theory; nonlinear disturbance observer; sea-skimming UAV; UAV

1. Introduction

A sea-skimming UAV is a specialized type of UAV, which is able to finish flight of short or long distance across sea surface with a certain low altitude above sea level [1]. On the contrary to the other UAVs, the flight height of sea-skimming UAV is at an obvious low zone, where the effect of sea waves and regarding to sea waves the sea condition cannot be ignored, sometimes it even may have to finish a steep descent stage [2] or be faced with the ground effect [3]. Under certain sea conditions the height of sea waves may have such serious effect that the measured distance between UAV and sea surface will obtain a nonneglected error/bias [4]. Hence, designing an effective method to reject/counteract external disturbances has become a significant and promising research focus.

*Corresponding author, Ph.D., E-mail: briansjmoma@outlook.com
[a] Professor, E-mail: ms.selezneva@bmstu.ru

ISSN: 2287-528X (Print), 2287-5271 (Online)

Nowadays, focuses of researches are mostly on filters or linear systems. For example, work of [4] utilizes a predictive filter to estimate the relative distance between UAV and sea surface, and [5] also take extended Kalman filter into account to design an altitude controller for sea-skimming UAVs. Their works have practical meaning: they regard the disturbance of sea wave as noise signals, based on which they present into algorithm filters to smooth these noises. However, filtering methods treat disturbances as noise for smoothing, but it is difficult to cope with the deterministic, large-amplitude, and low-frequency disturbances caused by sea waves. [6] tried to introduce an altitude combined filter in order to fit different stages of flight, and [7] designed an optimized hybrid filter system. However, once filter is considered, one has to think about its properties, sometimes in a perspective of statistic. Other works [8], [9], [10], [11], [12] choose to utilize adaptive theory combined with other control theories on UAV. It is a workable method, while adaptive law requires the adjustments of more parameters, which makes the parameter tuning a difficult task. Others proposed control methods based on modern control theory, like [13] proposed a Backstepping method, Qin et al. [14] also utilized Backstepping method but only on supercavitating vehicles; Zhou et al. [15], [16] applied super-twisting sliding mode control for high-speed vehicles and UAVs; these researches focused more on modern control theory itself other than disturbance-resisting solutions, or only considered ideal disturbances without random signals or high signal-to-noise ratio.

In this paper, we regard the disturbance as a centralized term that can be observed and compensated, and thus we propose a nonlinear-disturbance-observer-augmented Backstepping control method (NDOAB) in order to compensate the external disturbance. This architecture has the following advantages:

1) Decoupling design: The controller design and nonlinear disturbance observer (NDO) are relatively independent, which simplifies stability analysis and parameter adjusting.
2) Efficiency of calculation: The NDO has a simple structure and is easy to implement on the airborne computing platform.
3) Strong robustness: The proposed NDOAB control method can provide theoretical stability guarantee for bounded disturbances and performance robustness.

We first design a Backstepping controller without considering disturbance and prove its stability. Afterwards we take disturbance into account and renew the Backstepping control signal, based on which we redesign Lyapunov function and finish its proof on stability. It is proved that with the help of NDO our system will reach a uniformly exponential stability and is final consistent bounded. Related simulation results are shown in figures.

This paper contains following sections:

1) Mathematical model of sea-skimming fixed-wing UAV and its dynamical maneuvers;
2) Introduction and design of disturbance observer;
3) Design of controlling signals without and with consideration of disturbance from sea waves;
4) Proof of stability based on the meaning of Lyapunov theory;
5) Simulation and results.

2. Model of problem

2.1 Model of UAV

In this paper, a sea-skimming UAV is considered as a fixed-wing unmanned aerial vehicle. According to Newton's dynamic law, the movement of UAV could be described as follows in the form of grouped physical parameters

$$\begin{aligned}\dot{\boldsymbol{X}}_1 &= \boldsymbol{f}_1(V,\gamma,\chi)\\ \dot{\boldsymbol{X}}_2 &= \boldsymbol{f}_2(\alpha,\beta,\gamma,\mu,V,L,Y,D,T)\\ \dot{\boldsymbol{X}}_3 &= \boldsymbol{f}_3(\alpha,\beta,\gamma,\mu,p,q,r,L,Y,T)\\ \dot{\boldsymbol{X}}_4 &= \boldsymbol{f}_4(p,q,r,V,\delta_a,\delta_e,\delta_r)\end{aligned}$$

where $\boldsymbol{X}_1=[x \quad y \quad h]^T$, $\boldsymbol{X}_2=[V \quad \gamma \quad \chi]^T$, $\boldsymbol{X}_3=[\alpha \quad \beta \quad \mu]^T$, $\boldsymbol{X}_4=[p \quad q \quad r]^T$. x, y, h – position coordinates, V – velocity, γ – flight-path angle, χ – heading angle, α – attack angle, β – angle of sideslip, μ – roll angle, p, q, r – angular velocities, L – lift, Y – side load, D – resistance, T – thrust, $\delta_a,\delta_e,\delta_r$ – rudder control angles of fixed-wing UAV.

These dynamic equations can be rewritten in the following expanded form

$$\begin{cases}\dot{x}=V\cos\chi\cos\gamma\\ \dot{y}=V\sin\chi\cos\gamma\\ \dot{h}=-V\sin\gamma\\ \dot{V}=\dfrac{T\cos\alpha\cos\beta-D}{m}-g\sin\gamma\\ \dot{\gamma}=\dfrac{T(\sin\alpha\cos\mu+\cos\alpha\sin\beta\sin\mu)}{mV}+\dfrac{L\cos\mu-Y\sin\mu}{mV}-\dfrac{g\cos\gamma}{V}\\ \dot{\chi}=\dfrac{T(\sin\alpha\sin\mu-\cos\alpha\sin\beta\cos\mu)}{mV\cos\gamma}+\dfrac{L\sin\mu+Y\cos\mu}{mV\cos\gamma}\\ \dot{\Theta}=q\\ \dot{\alpha}=q-\dot{\gamma}=-\dfrac{L}{mV\cos\beta}+\dfrac{g\cos\gamma\cos\mu}{V\cos\beta}-\dfrac{\sin\alpha}{\cos\beta}T-p\tan\beta\cos\alpha+q-r\sin\alpha\tan\beta\\ \dot{\beta}=\dfrac{Y}{mV}+\dfrac{g}{V}\cos\gamma\sin\mu-T\cos\alpha\sin\beta+p\sin\alpha-r\cos\alpha\\ \dot{\mu}=\dfrac{Y\tan\gamma\cos\mu}{mV}+\dfrac{L(\tan\beta+\tan\gamma\sin\mu)}{mV}-\dfrac{g\tan\beta\cos\gamma\cos\mu}{V}\\ \quad +T(\tan\beta\sin\alpha-\tan\gamma\cos\mu\cos\alpha\sin\beta+\tan\gamma\sin\alpha\sin\mu)\\ \quad +p\sec\beta\cos\alpha+r\sec\beta\sin\alpha\\ \dot{p}=\Gamma_3M_{l0}+\Gamma_4M_{n0}+\Gamma_1pq-\Gamma_2qr+\bar{q}b\left(\Gamma_3C_{l\delta_a}+\Gamma_4C_{n\delta_a}\right)\cdot\delta_a+\bar{q}b\left(\Gamma_3C_{l\delta_r}+\Gamma_4C_{n\delta_r}\right)\cdot\delta_r\\ \dot{q}=\Gamma_9M_{m0}+\Gamma_5pr-\Gamma_6(p^2-r^2)+\bar{q}c\Gamma_9C_{m\delta_e}\cdot\delta_e\\ \dot{r}=\Gamma_4M_{l0}+\Gamma_8M_{n0}+\Gamma_7pq-\Gamma_1qr+\bar{q}b\left(\Gamma_4C_{l\delta_a}+\Gamma_8C_{n\delta_a}\right)\cdot\delta_a+\bar{q}b\left(\Gamma_4C_{l\delta_r}+\Gamma_8C_{n\delta_r}\right)\cdot\delta_r,\end{cases}\tag{1}$$

where m and Θ are the mass and pitch angle of UAV respectively; $\Gamma_i(i=1,\cdots,9)$ and $\bar{q}$ have the following forms, in which J_x, J_y, J_z, J_{xz} are moments of inertia

$$\begin{aligned}&\Gamma_1=\frac{J_{xz}(J_x-J_y+J_z)}{\Gamma},\Gamma_2=\frac{J_z(J_z-J_y)+J_{xz}^2}{\Gamma}\\ &\Gamma_3=\frac{J_z}{\Gamma},\Gamma_4=\frac{J_{xz}}{\Gamma},\Gamma_5=\frac{J_z-J_x}{J_y},\Gamma_6=\frac{J_{xz}}{J_y}\\ &\Gamma_7=\frac{J_z(J_x-J_y)+J_{xz}^2}{\Gamma},\Gamma_8=\frac{J_x}{\Gamma},\Gamma_9=\frac{1}{J_y}\\ &\Gamma=J_xJ_z-J_{xz}^2,\qquad \bar{q}=\frac{1}{2}\rho V^2S\end{aligned},$$

In order to simplify the fitting of aerodynamic coefficients, one most popular way is to ignore higher-order terms and to take into account simplified fitted aerodynamic coefficients. Thus the lift, side load, resistance and the aerial moments denote [17]

$$\begin{aligned} L &= \bar{q}C_L(\delta_e,\alpha) = \bar{q}\left(C_{L0} + C_{L\alpha}\alpha + C_{L\delta_e}\cdot\delta_e\right) \\ Y &= \bar{q}C_Y(\beta) = \bar{q}\left(C_{Y0} + C_{Y\beta}\beta\right) \\ D &= \bar{q}C_D(\alpha) = \bar{q}(C_{D0} + C_{D\alpha}\alpha) \end{aligned}, \tag{2}$$

$$\begin{aligned} M_l &= \bar{q}b\left(C_{l\beta}\beta + C_{lp}\frac{bp}{2V} + C_{lr}\frac{br}{2V} + C_{l\delta_a}\delta_a + C_{l\delta_r}\delta_r\right) \\ M_m &= \bar{q}c\left(C_{m0} + C_{m\alpha}\alpha + C_{mq}\frac{cq}{2V} + C_{m\delta_e}\delta_e\right) \\ M_n &= \bar{q}b\left(C_{n\beta}\beta + C_{np}\frac{bp}{2V} + C_{nr}\frac{br}{2V} + C_{n\delta_a}\delta_a + C_{n\delta_r}\delta_r\right) \end{aligned}, \tag{3}$$

where ρ – density of air, S – relative area of UAV's wing, $C_L(\delta_e,\alpha)$ – lift coefficient, $C_Y(\beta)$ – sideslip coefficient, $C_D(\alpha)$ – drag coefficient, δ_e – elevator deflection, C_{L0}, C_{Y0}, C_{D0} – constants; b, c – characteristic lengths; $C_{l,i}, C_{n,i}(i = \beta, p, r, \delta_a, \delta_r)$ and $C_{m0}, C_{m\alpha}, C_{mq}, C_{m\delta_e}$ are aerodynamic parameters.

When focusing on vertical channel (pitch and height), UAV moves alongside axis x and other sideslip movements are ignored, i.e., $\beta, \mu, Y, \chi, p, r = 0$. Since we shall not apply controls on sideslip movements, $\delta_a, \delta_r = 0$. Thus, upper Eq. (1) can denote as Eq. (4).

$$\begin{cases} \dot{x} = V\cos\gamma \\ \dot{h} = -V\sin\gamma \\ \dot{V} = \frac{T\cos\alpha - D}{m} - g\sin\gamma \\ \dot{\gamma} = \frac{T\sin\alpha + L}{mV} - \frac{g\cos\gamma}{V} \\ \dot{\chi} = \frac{Y}{mV\cos\gamma} \\ \dot{\Theta} = q \\ \dot{\alpha} = -\frac{L}{mV} + \frac{g\cos\gamma}{V} - T\sin\alpha + q \\ \dot{q} = \Gamma_9 M_{m0} + \bar{q}c\Gamma_9 C_{m\delta_e}\cdot\delta_e \\ \dot{y} = \dot{\beta} = \dot{\mu} = \dot{p} = \dot{r} = 0 \end{cases}, \tag{4}$$

From Eq. (4) we can come to the conclusion that the adjustment of flight height can be realized by controlling elevator deflection δ_e, since the lift corresponds only with it. Based on this conclusion the elevator deflection δ_e shall be selected as controlling signal. In this paper we consider only vertical movements along the axis h, in this case Eq. (2) denotes Eq. (5).

$$\begin{aligned} L &= \bar{q}C_L(\alpha) \approx \bar{q}(C_{L0} + C_{L\alpha}\alpha) \\ D &= \bar{q}C_D(\alpha) \approx \bar{q}(C_{D0} + C_{D\alpha}\alpha)' \end{aligned} \tag{5}$$

2.2 Model of sea waves

The sea waves can be regarded as series of randomly combined sinusoid signals, given the fact that the amplitude and frequency of wave depend largely on researched sea situation. According to work of [18], different sea situations can be described as the following Table 1

Table 1. Sea conditions and their sea wave heights

Condition	1-2	3	4	5	6	7	8
Height, m	0-0.5	0.5-1.25	1.25-2.5	2.5-4	4-6	6-9	9-14

There are actually several ways to propose sea waves models. Some researches prefer to describe them as a single sinusoidal wave with a certain height and certain frequency, for example the Gerstner model and JONSWAP spectrum [19]; some more complicated researches propose the widely used Pierson-Moskowitz spectrum to generate the simulated sea waves [20]; other possible ways to simulate sea waves are superposition of sinusoidal waves [21], synchronizing of low and high spectrums [22], Longuet-Higgins model [23], simulation waves nearshore [24] and so on. Among all the above methods the JONSWAP spectrum method has a broad use in researches and practical usages, thus in this paper alternatively the simulation of different waves is calculated by JONSWAP spectrum.

The JONSWAP spectrum theory was founded in a measurement program in the North Sea between Germany and Iceland in 1968-1969 years, which was named as "Joint North Sea Wave Project" (JONSWAP). The results have been adopted as the ITTC standard and are meaningful to represent sea waves generated by winds under limited water depth [25]. The spectral density of sea waves can be written as

$$\begin{aligned} S_1(\omega) &= 155\frac{H_s^2}{T_1^4\omega^5}\exp\left(\frac{-944}{T_1^4\omega^4}\right)\gamma^{Y_1} \\ Y_1 &= \exp\left[-\left(\frac{0.191\omega T_1-1}{\sqrt{2}\sigma}\right)^2\right] \end{aligned}, \tag{6}$$

$$\begin{aligned} S_2(\omega) &= \frac{\alpha g^2}{(2\pi)^4 f^5}\exp\left[-1.25\left(\frac{f}{f_p}\right)^{-4}\right]\gamma^{Y_2}, \\ Y_2 &= \exp\left[-0.5\left(\frac{f-f_p}{\sigma f_p}\right)^2\right], \end{aligned} \tag{7}$$

Eq. (6) and Eq. (7) are equivalent in describing sea waves via frequency ω or f. Here in Eq. (6) ω is the frequency of sea waves, T_1 is the average wave period, H_s is the significant sea wave height, γ is constant (usually be taken as $\gamma = 3.3$), σ is constant also (usually $\sigma = 0.07$ or $\sigma = 0.09$); in Eq. (7) f_p is peak frequency, f is sea wave period; α is constant and its value satisfies $H_s = 4\sqrt{m_0}$ with m_0 being the zero-order moment of spectrum [26]. Considering achievability we utilize Eq. (7) to simulate the sea waves. The relative parameters are shown later in Section 6.

In Fig. 1 we present examples of sea waves of conditions 7, 5, 4, generated by Eq. (6). It should be noticed that the sea conditions in Table 1 describes significant wave height, which is the average height of the highest one-third of the waves. Generally the maximum height of waves is higher than significant wave height, i.e., $H_{\max} = (1.6\sim1.8)H_{\text{sig}}$.

2.3 Flight altitude and attitude model with disturbance of sea waves

Originally it is reasonable for a sea-skimming UAV to divide its flight process into three stages: launch stage, cruise stage, target stage. At launch stage a UAV is launched from a certain kind of

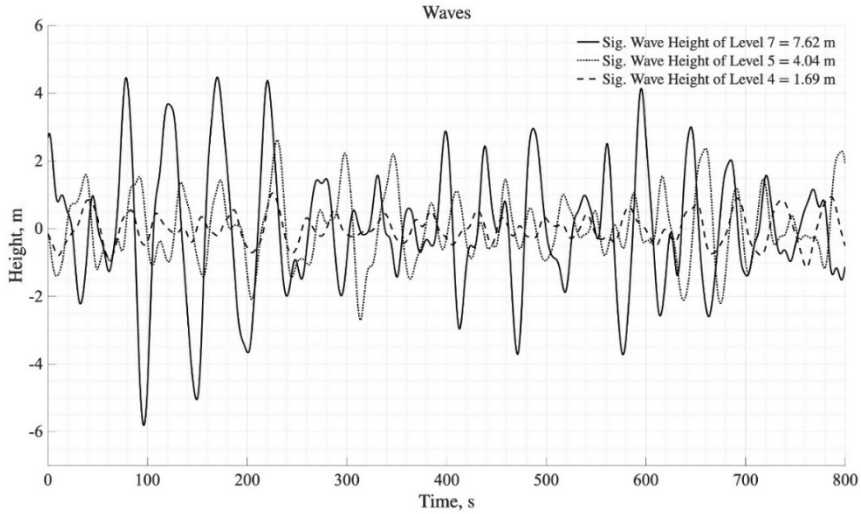

Figure 1. Examples of sea waves of conditions 7, 5, 4

platform in order to gain an initial velocity and initial height. At cruise stage a UAV usually flies with certain velocity and height, and at this stage UAV will seldom finish manoeuvres in order to save fuel. But in some occasions UAV will change its flight height to avoid detection. At target stage UAV will finish target manoeuvres or land at target point. Obviously, the ability to descend from the initial height to a desired height smoothly and stably presents a challenging point for UAV [2].

Nowadays existing literatures focus on control algorithms under steady flights – in other words flights where height of sea waves can be ignored. In these situations, sea-skimming flight can be regarded as ordinary flight, control algorithm of which is simpler, respectively. In this paper the height of sea wave will be considered, as a result of which we detailly established the model of flight height (Fig. 2). Assuming the measured height at launch point is the initial height h_0, then the sea level at launch point can be considered as the initial sea level with the altitude of 0m. We assume that the sea wave higher than the initial sea level has positive value $\eta > 0$, and the sea wave lower than the initial level has negative value $\eta < 0$, thereby the actual height h shall be described as follows

$$h = h_{cal} - \eta, \tag{8}$$

here h is the actual height relative to local sea wave, h_{cal} is the calculated height relative to initial sea level (we consider the initial level as 0 m), η is the height of sea wave. Eq. (8) gives us relatively real value of actual height.

Taking into account the influence of sea wave, we can mathematically get the first and second derivative of flight height based on Eq. (4). Aligned with Eq. (5) we shall substitute them and get

$$\begin{aligned} \ddot{h} &= \frac{D\sin\gamma - \bar{q}(C_{L0} + C_{L\alpha}\alpha)\cos\gamma}{m} + g - \frac{1}{m}T\sin\Theta - \ddot{\eta} \\ &= f_h(V, \alpha, \gamma) + g_{hT}(\Theta)T + d \end{aligned}, \tag{9}$$

where $d = -\ddot{\eta}$.

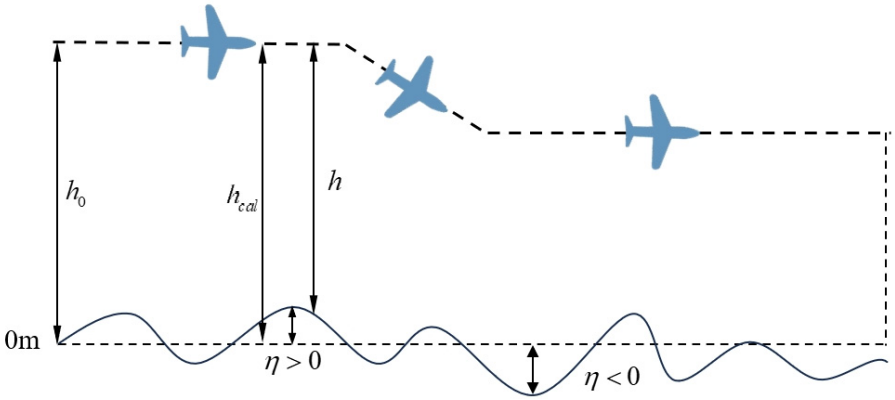

Figure 2. Model of flight height

On the other hand, from Eq. (4) we shall get the attitude movement of pitch angle

$$\begin{aligned}\ddot{\Theta} = \dot{q} &= \Gamma_9 M_{m0} + \bar{q} c \Gamma_9 C_{m\delta_e} \cdot \delta_e \\ &= f_\Theta(\alpha, q) + g_{\Theta\delta_e}(V)\delta_e\end{aligned}, \tag{10}$$

Eq. (9) and Eq. (10) denote the vertical movement of UAV.

3. Design of backstepping control method

Assuming the desired flight height as h_d, the desired pitch angle as Θ_d, we can establish the state vectors as follows

$$\boldsymbol{X}_{1d} = \begin{bmatrix} h_d \\ \Theta_d \end{bmatrix}, \quad \boldsymbol{X}_1 = \begin{bmatrix} h \\ \Theta \end{bmatrix}, \quad \boldsymbol{X}_2 = \begin{bmatrix} \dot{h} \\ \dot{\Theta} \end{bmatrix}, \quad \boldsymbol{U} = \begin{bmatrix} T \\ \delta_e \end{bmatrix},$$
$$\boldsymbol{F}(V, \alpha, \gamma, q) = \begin{bmatrix} f_h \\ f_\Theta \end{bmatrix}, \quad \boldsymbol{G}(V, \Theta) = \begin{bmatrix} g_{hT} & 0 \\ 0 & g_{\Theta\delta_e} \end{bmatrix}$$
$$\dot{\boldsymbol{X}}_1 = \boldsymbol{X}_2, \quad \dot{\boldsymbol{X}}_2 = \boldsymbol{F}(V, \alpha, \gamma, q) + \boldsymbol{G}(V, \Theta)\boldsymbol{U}$$

Theorem 1: for the sea-skimming situation discussed in this paper, the UAV will obtain its flight stability without consideration of external disturbance, only when the control thrust and elevator deflection claim as follows, s.t. $\boldsymbol{K}_1, \boldsymbol{K}_2 > 0$

$$\boldsymbol{U} = \begin{bmatrix} T \\ \delta_e \end{bmatrix} = \boldsymbol{G}^{-1}(V, \Theta)\left[-\boldsymbol{F}(V, \alpha, \gamma, q) + \ddot{\boldsymbol{X}}_{1d} - \boldsymbol{d} - \boldsymbol{K}_1(\boldsymbol{e}_2 + \boldsymbol{K}_1\boldsymbol{e}_1) + \boldsymbol{e}_1 - \boldsymbol{K}_2\boldsymbol{e}_2\right], \tag{11}$$

where $\boldsymbol{e}_1 = \boldsymbol{X}_{1d} - \boldsymbol{X}_1 = [e_h \quad e_\Theta]^T$ is the error between desired state (height and pitch angle) and actual state, $\boldsymbol{e}_2 = \boldsymbol{X}_2 - \dot{\boldsymbol{X}}_{1d} - \boldsymbol{K}_1\boldsymbol{e}_1 = [e_{2u} \quad e_{2d}]^T$ is the auxiliary error item; the matrices $\boldsymbol{K}_1, \boldsymbol{K}_2 \in \mathbb{R}^{2\times 2}$ are symmetric and diagonal, i.e., $\boldsymbol{K}_1 = \mathrm{diag}(\alpha_1, \alpha_2)$, $\boldsymbol{K}_2 = \mathrm{diag}(\alpha_3, \alpha_4)$. Meanwhile the disturbance matrix $\boldsymbol{d} = [d \quad 0]^T$ since the sea wave disturbance affects only the height of UAV with the second component of zero.

Proof. Claim a Lyapunov function and its derivative

$$V = \frac{1}{2}\boldsymbol{e}_1^T\boldsymbol{e}_1,$$
$$\dot{V} = \boldsymbol{e}_1^T\dot{\boldsymbol{e}}_1 = \boldsymbol{e}_1(\dot{\boldsymbol{X}}_{1d} - \dot{\boldsymbol{X}}_1) = \boldsymbol{e}_1(\dot{\boldsymbol{X}}_{1d} - \boldsymbol{X}_2)$$

On this step we can control the Lyapunov function only by controlling $\boldsymbol{X}_2$. With the target of setting $\dot{V} < 0$ the measured height should have followed form (we mark it as $\boldsymbol{X}_2^v$):

$$\boldsymbol{X}_2^v = \dot{\boldsymbol{X}}_{1d} + \boldsymbol{K}_1\boldsymbol{e}_1 \qquad (\boldsymbol{K}_1 > 0)$$

Thus, the derivative of Lyapunov function shall be smaller than zero and the UAV will obtain flight stability

$$\dot{V} = \boldsymbol{e}_1(\dot{\boldsymbol{X}}_{1d} - \boldsymbol{X}_2^v) = -\boldsymbol{e}_1^T\boldsymbol{K}_1\boldsymbol{e}_1 < 0$$

Unfortunately, the actual value of $\boldsymbol{X}_2^v$ doesn't match the value we designed above. In this sense $\boldsymbol{X}_2^v$ represents the virtual control. Thus, we have to claim the error between derivative of actual value $\boldsymbol{X}_2$ and virtual control $\boldsymbol{X}_2^v$ as an augmented (auxiliary) item

$$\boldsymbol{e}_2 = \boldsymbol{X}_2 - \boldsymbol{X}_2^v = \boldsymbol{X}_2 - \dot{\boldsymbol{X}}_{1d} - \boldsymbol{K}_1\boldsymbol{e}_1$$

In this case we get $\dot{\boldsymbol{X}}_{1d} - \boldsymbol{X}_2 = -\boldsymbol{K}_1\boldsymbol{e}_1 - \boldsymbol{e}_2$. Taking into account the error $\boldsymbol{e}_2$ we shall organize augmented Lyapunov function and its derivative

$$\begin{aligned} V &= \frac{1}{2}\boldsymbol{e}_1^T\boldsymbol{e}_1 + \frac{1}{2}\boldsymbol{e}_2^T\boldsymbol{e}_2, \\ \dot{V} &= \boldsymbol{e}_1^T\dot{\boldsymbol{e}}_1 + \boldsymbol{e}_2^T\dot{\boldsymbol{e}}_2 \\ &= \boldsymbol{e}_1^T(\dot{\boldsymbol{X}}_{1d} - \boldsymbol{X}_2) + \boldsymbol{e}_2^T(\dot{\boldsymbol{X}}_2 - \ddot{\boldsymbol{X}}_{1d} - \boldsymbol{K}_1\dot{\boldsymbol{e}}_1) \\ &= -\boldsymbol{e}_1^T(\boldsymbol{K}_1\boldsymbol{e}_1 + \boldsymbol{e}_2) + \boldsymbol{e}_2^T[\boldsymbol{F}(V,\alpha,\gamma,q) + \boldsymbol{G}(V,\Theta)\boldsymbol{U} - \ddot{\boldsymbol{X}}_{1d} + \boldsymbol{K}_1(\boldsymbol{K}_1\boldsymbol{e}_1 + \boldsymbol{e}_2)] \end{aligned}$$

Since the Lyapunov function is influenced only by control signal $\boldsymbol{U}$, we can take the designed control Eq. (11) into account and get

$$\dot{V} = -\boldsymbol{e}_1^T\boldsymbol{K}_1\boldsymbol{e}_1 - \boldsymbol{e}_2^T\boldsymbol{K}_2\boldsymbol{e}_2 < 0$$

By meaning of Lyapunov theory, system will be stable. This ends the proof.

Considering that the height and pitch movements of UAV are not coupled, it's more practical to separately calculate control signals on each channel from Eq. (11)

$$T = \frac{1}{g_{hT}}[-f_h + \ddot{h}_d - d - \alpha_1(\alpha_1 e_h + e_{2u}) + e_h - \alpha_3 e_{2u}], \tag{12}$$

$$\delta_e = \frac{1}{g_{\Theta\delta_e}}[-f_\Theta + \ddot{\Theta}_d - \alpha_2(\alpha_2 e_\Theta + e_{2d}) + e_\Theta - \alpha_4 e_{2d}], \tag{13}$$

4. Design of nonlinear disturbance observer

Nonlinear disturbance observer (NDO) is regarded as an effective way to estimate and compensate disturbance in system and to achieve improved performance of it. Compared with the so-called extended state observer (ESO) [27], [28], [29], [30], NDO has simpler structure and vectors with lower dimensions [31], [32], [33], [34]), which benefits the calculation on UAV. For a system which has the following standard Cauchy form with $\boldsymbol{X} = [x_1 \quad x_2]^T$

$$\begin{cases}\dot{x}_1 = x_2 \\ \dot{x}_2 = f(t,\boldsymbol{X}) + g(t,\boldsymbol{X})U + d\end{cases}, \tag{14}$$

one can design a disturbance observer with the coefficient L [32]

$$\begin{cases}\dot{z} = -L(\boldsymbol{X})z - L(\boldsymbol{X})\big(L(\boldsymbol{X})x_2 + f(t,\boldsymbol{X})\big) - L(\boldsymbol{X})g(t,\boldsymbol{X})U \\ \hat{d} = z + L(\boldsymbol{X})x_2\end{cases}, \tag{15}$$

where z is the state of the observer, $L(\boldsymbol{X})$ is the coefficient function, $\hat{d}$ is the estimation of the disturbance d. According to the dimension of x, f, U, d the coefficient function $L(\boldsymbol{X})$ could take with different dimensions. In this paper given to the fact that we research on the altitude channel of UAV, here $L(\boldsymbol{X}) \in \mathbb{R}^1$ is a scalar function.

Assumption 1: it is assumed that the derivative of disturbance $\dot{d}$ shall satisfy $|\dot{d}| < \psi$, where $\psi > 0$ is a constant.

Assumption 1 indicates that the velocity of disturbance is bounded. It explains the practical realizability of designed later algorithm, because during the flight of UAV the height of sea waves present themselves with a continuous wave signal, which indicates the derivative of their height is bounded and have the upper range.

Assumption 2: the coefficient function $L(\boldsymbol{X})$, its derivative and the velocity x_2 are bounded, i.e. $L(\boldsymbol{X}) \geq L_{\min} > 0$, $|\dot{L}(\boldsymbol{X})| \leq \rho$, $|x_2| \leq M$.

Assumption 2 indicates that the changing rate of coefficient function and velocity of height should not be infinite, which is in line with the reality, given the fact that the NDO estimates the disturbances only with a continuous coefficient function, and the flight velocity practically will not sharply change its value. Additionally, we give the lower bound of coefficient function in order to get a better dynamic process, and the stability analysis will be conducted later.

Theorem 2: the designed state observer Eq. (15) will guarantee the estimation of external disturbance on the base of Lyapunov meaning, and meanwhile holds its stability during the process of estimation.

Proof. Assume the NDO error as $\tilde{d} = d - \hat{d}$. We can get the derivative of the NDO error as

$$\begin{aligned}\dot{\tilde{d}} &= \dot{d} - \dot{\hat{d}} \\ &= \dot{d} - \dot{z} - \dot{L}(\boldsymbol{X})x_2 - L(\boldsymbol{X})\dot{x}_2 \\ &= \dot{d} + L(\boldsymbol{X})z + L(\boldsymbol{X})\big(L(\boldsymbol{X})x_2 + f(t,\boldsymbol{X})\big) + L(\boldsymbol{X})g(t,\boldsymbol{X}) - \dot{L}(\boldsymbol{X})x_2 \\ &\quad -L(\boldsymbol{X})(f(t,\boldsymbol{X}) + g(t,\boldsymbol{X})U + d) \\ &= \dot{d} + L(\boldsymbol{X})(z + L(\boldsymbol{X})x_2) - \dot{L}(\boldsymbol{X})x_2 - L(\boldsymbol{X})d \\ &= \dot{d} + L(\boldsymbol{X})\hat{d} - \dot{L}(\boldsymbol{X})x_2 - L(\boldsymbol{X})d \\ &= \dot{d} - L(\boldsymbol{X})\tilde{d} - \dot{L}(\boldsymbol{X})x_2\end{aligned}, \tag{16}$$

Claim a Lyapunov function and get its derivative

$$V = \frac{1}{2}\tilde{d}^2, \tag{17}$$

$$\begin{aligned}\dot{V} &= \tilde{d}\dot{\tilde{d}} \\ &= \tilde{d}\big(\dot{d} - L(\boldsymbol{X})\tilde{d} - \dot{L}(\boldsymbol{X})x_2\big) \\ &= -L(\boldsymbol{X})\tilde{d}^2 + \tilde{d}\big(\dot{d} - \dot{L}(\boldsymbol{X})x_2\big)\end{aligned}, \tag{18}$$

considering that $L(\boldsymbol{X}) > L_{\min} > 0$ in Assumption 2 we have

$$\begin{aligned}\dot{V} &= -L(\boldsymbol{X})\tilde{d}^2 + \tilde{d}\left(\dot{d} - \dot{L}(\boldsymbol{X})x_2\right)\\ &\le -L(\boldsymbol{X})\tilde{d}^2 + \tilde{d}(\psi + \rho M)\\ &\le -L_{\min}\tilde{d}^2 + \left|\tilde{d}\right|(\psi + \rho M)\end{aligned}$$

let $\delta = \frac{\psi+\rho M}{L_{\min}}$. The system obviously turns into

$$\dot{V} \le -L_{\min}\tilde{d}^2 + \left|\tilde{d}\right|(\psi + \rho M) = -L_{\min}\left(\tilde{d}^2 - \delta\left|\tilde{d}\right|\right)$$

Consider the following set

$$\mathcal{S} = \{\tilde{d}\,|\,|\tilde{d}| \ge \delta\}, \tag{19}$$

when $\tilde{d}$ is in $\mathcal{S}$, $\dot{V} \le -L_{\min}\left(\tilde{d}^2 - \delta\left|\tilde{d}\right|\right) \le 0$, according to Lyapunov theory, derivative of Lyapunov function is strictly non-positive, the NDO will hold its stability.

As for $\tilde{d} \in \bar{\mathcal{S}}$ ($\bar{\mathcal{S}}$ is the complement set of $\mathcal{S}$), $\dot{V} \ge 0$, leading to the rising of $\tilde{d}$ until $\left|\tilde{d}\right| > \delta$; at this moment $\tilde{d}$ falls back into set $\mathcal{S}$, which gives $\dot{V} \le 0$, thus system is stable. Thus, the NDO is stable and uniformly bounded in a certain bound, i.e. the NDO is final consistent bounded. This ends the proof.

Remark 1: Throughout Eqs. (16)-(19) there is no requirements on $L(\boldsymbol{X})$ except for its boundedness. Thus in this paper we design $L(\boldsymbol{X})$ as follows

$$\begin{aligned}L(\boldsymbol{X}) &= L_0\alpha_h\alpha_{\dot{h}}\\ \alpha_h &= \frac{1}{1+K_h|e_1|}\\ \alpha_{\dot{h}} &= \frac{1}{1+K_{\dot{h}}|\dot{h}|}\end{aligned}, \tag{20}$$

where $K_h, K_{\dot{h}} > 0$ are constants, $e_1 = h - h_d$ is the error between actual height and desired height; $L_0 > 0$ is the upper bound of $L(\boldsymbol{X})$. One can easily notice that $0 < \alpha_h, \alpha_{\dot{h}} \le 1$, thus the coefficient function $L(\boldsymbol{X})$ is bounded in $0 < L(\boldsymbol{X}) < L_0$, which can automatically adjust its value based on e_1 and $\dot{h}$ – the larger the error or the height velocity, the smaller $L(\boldsymbol{X})$, creating a quasi-adaptive coefficient function. The changes of $L(\boldsymbol{X})$ will be shown later in Section 6.

5. Consideration of evaluated disturbance based on NDO

Eq. (12) gives the Backstepping control of thrust T considering the actual disturbance of sea waves. However, for a UAV in practical situations only evaluated disturbance $\hat{d}$ can be taken into account, thus the difference of disturbance is brought into system. As is shown in Eq. (11) $\boldsymbol{d} = [d \quad 0]^T$, the height of sea waves affects only the flight height of UAV, we will take the compensatory measures especially for height channel, i.e., for thrust T.

Theorem 3: The considered system of UAV with the skimming-sea flight holds its stability, if control thrust T is organized as follows, s.t. $\alpha_1, \alpha_2 > 0$

$$T = \frac{1}{g_{hT}}\left[-f_h + \ddot{h}_d - \hat{d} - \alpha_1(\alpha_1 e_h + e_{2u}) + e_h - \alpha_2 e_{2u}\right], \tag{21}$$

Proof. The existence of evaluated disturbance means the existence of the evaluation error, which is marked by $\tilde{d} = d - \hat{d}$. Compared with thrust Eq. (12), thrust Eq. (21) utilizes the estimation of disturbance $\hat{d}$ other than its real value. Changing the control thrust, one augmented Lyapunov function especially for height shall be reconsidered, including the estimation error $\tilde{d}$

$$V = \frac{1}{2}e_h^2 + \frac{1}{2}e_{2u}^2 + \frac{1}{2}\tilde{d}^2, \tag{22}$$

where $e_h = h_d - h$, e_{2u} is the first component of $\boldsymbol{e}_2 = \boldsymbol{X}_2 - \dot{\boldsymbol{X}}_{1d} - \boldsymbol{K}_1\boldsymbol{e}_1$.

Given the thrust control Eq. (21) and taking into consideration Assumption 1 and 2 we have

$$\begin{aligned}
\dot{V} &= -e_h(e_{2u} + \alpha_1 e_h) + \tilde{d}\dot{\tilde{d}} + e_{2u}\left[f_h + g_{hT}T + \hat{d} - \ddot{h}_d + \alpha_1(e_{2u} + \alpha_1 e_h)\right] \\
&= -\alpha_1 e_h^2 - \alpha_2 e_{2u}^2 + e_{2u}\tilde{d} + \tilde{d}\left(\dot{d} - L(\boldsymbol{X})\tilde{d}\right) - \tilde{d}\dot{L}(\boldsymbol{X})x_2 \\
&= -\alpha_1 e_h^2 - \alpha_2 e_{2u}^2 - L(\boldsymbol{X})\tilde{d}^2 + \tilde{d}\left(\dot{d} - \dot{L}(\boldsymbol{X})x_2\right) \\
&\le -\alpha_1 e_h^2 - \alpha_2 e_{2u}^2 - L(\boldsymbol{X})\tilde{d}^2 + \left|\tilde{d}\right|(\psi + \rho M) \\
&= -\alpha_1 e_h^2 - \alpha_2 e_{2u}^2 - L(\boldsymbol{X})\tilde{d}^2 + L_{\min}\left|\tilde{d}\right|\delta \\
&\le -\alpha_1 e_h^2 - \alpha_2 e_{2u}^2 - L(\boldsymbol{X})\tilde{d}^2 + L_{\min}\frac{\tilde{d}^2 + \delta^2}{2} \\
&\le -2\min\left\{\alpha_1, \alpha_2, L(\boldsymbol{X}) - \frac{1}{2}L_{\min}\right\}V + \frac{1}{2}L_{\min}\delta^2 \\
&= -\kappa_1 V + \zeta_1
\end{aligned}, \tag{23}$$

where $\kappa_1 = 2\min\left\{\alpha_1, \alpha_2, L(\boldsymbol{X}) - \frac{1}{2}L_{\min}\right\}$, $\zeta_1 = \frac{1}{2}L_{\min}\delta^2 = \frac{(\psi+\rho M)^2}{2L_{\min}}$.

For the set $\mathcal{W} = \left\{\left(e_h, e_{2u}, \tilde{d}\right)\middle||e_h|^2 + |e_{2u}|^2 + \left|\tilde{d}\right|^2 \ge 2\frac{\zeta_1}{\kappa_1}\right\}$, when $\left(e_h, e_{2u}, \tilde{d}\right) \in \mathcal{W}$

$$V = \frac{1}{2}e_h^2 + \frac{1}{2}e_{2u}^2 + \frac{1}{2}\tilde{d}^2 \ge \frac{\zeta_1}{\kappa_1} \Longrightarrow$$

$$\dot{V} \le -\kappa_1 V + \zeta_1 \le -\kappa_1 \cdot \frac{\zeta_1}{\kappa_1} + \zeta_1 = 0$$

Thus, Lyapunov function become non-positive and system is stable. Similarly when $\left(e_h, e_{2u}, \tilde{d}\right) \in \bar{\mathcal{W}}$ ($\bar{\mathcal{W}}$ is the complement of set $\mathcal{W}$), the Eq. (23) claims

$$V(t) = \frac{\zeta_1}{\kappa_1}(1 - e^{-\kappa_1 t}). \tag{24}$$

which indicates that the Lyapunov function will exponentially converge to $\mathcal{W}$ with the rate of $e^{-\kappa_1 t}$, holding the upper bound of $\lim_{t\to\infty}\sup_{V\in\bar{\mathcal{W}}} V(t) = \frac{\zeta_1}{\kappa_1}$. Thus the system is final consistent bounded [35]. This ends the proof.

In next chapter we will utilize the control thrust in Eq. (21) and controlling elevator deflection in Eq. (13) to fulfil the simulation.

6. Simulations and results

In this paper we focus on a certain type of fixed-wing UAV and in Table 2 its parameters for simulation are listed. Other than that, we use parameters in Table 3 for sea wave simulation, regarding Eq. (7).

Table 2. Parameters of UAV

m, kg	13	C_{m0}	-0.02
S, m^2	0.63	$C_{m\alpha}$	-0.41
$\rho, \mathrm{kg/m}^3$	1.27	C_{mq}	-3.8
$J_y, \mathrm{kg \cdot m}^2$	1.129	$C_{m\delta_e}$	-0.5
C_{D0}	0.03	c	0.18
$C_{D\alpha}$	0.30	h_d, m	15
C_{L0}	0.27	$\bar{T}$	800
$C_{L\alpha}$	3.4	$\bar{\delta}_e$	30°

Table 3. Parameters of JONSWAP spectrum method

Sea states	Level 7	Level 5	Level 4
γ		3.3	
$g, \mathrm{m/s}^2$		9.81	
f_p		0.02	
σ		0.07	
α	2×10^{-6}	1.3×10^{-5}	3.4×10^{-5}
H_s, m	8	5	2
Simulated $H_{s,sim}, \mathrm{m}$	7.62	4.04	1.69

Table 4. Parameters of NDOAB method

Sea states	Level 7	Level 5	Level 4
α_1 of T		6	
α_3 of T		2	
α_2 of T		5	
α_4 of T		12	
L_0		2	
K_h	0.3	0.5	0.5
$K_{\dot{h}}$	0.05	0.03	0.03

Design the coefficient of proposed NDOAB method as given in Table 4, according to Eq. (13), Eq. (20) and Eq. (21).

Fig. 3 shows the height trajectory along the h-axis, in which the control algorithm is processed without NDO. The sea condition is of level 7, where significant sea wave height is 7.62 m. It is obvious that fixed-wing UAV flies along an unstable and unsmooth trajectory, which presents frequent oscillations in height. The descent stage of desired trajectory pulls in distance from the UAV to sea level, whereas the influence of disturbance (sea waves height) enhances, considering the SNR from 7.62/50 = 15.24% to 7.62/15 = 50.8%. Without NDO we shall not claim the extended state and its estimation, so the lack in disturbance resistance method leads to severe trajectory oscillation or even crush. On the other hand, despite of the crushing risk, during its flight

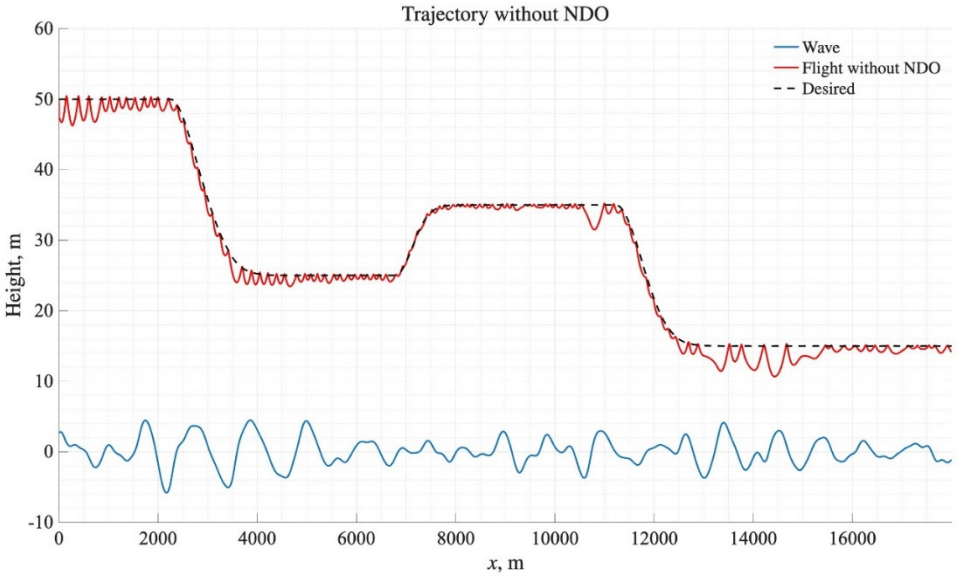

Figure 3. Height trajectory without NDO

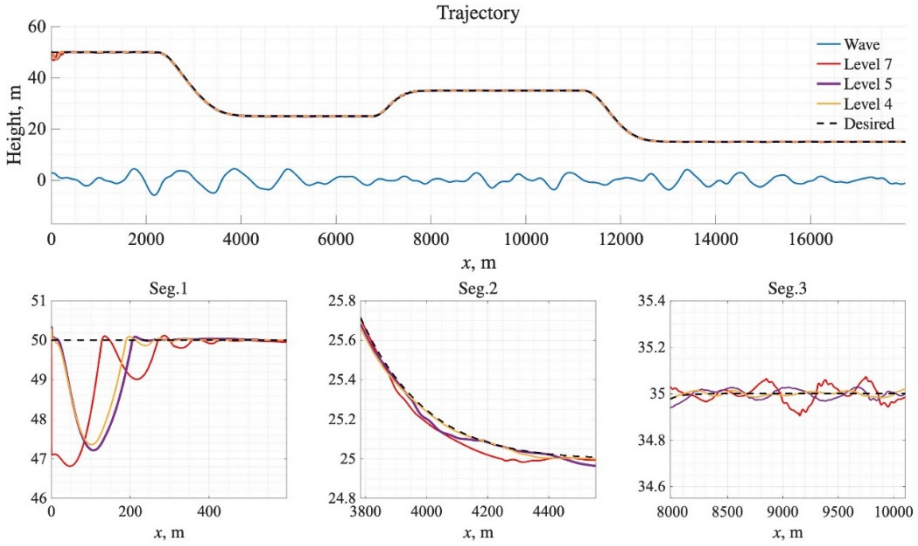

Figure 4. Trajectories under sea conditions of levels 7, 5, 4

the tracking error once reaches 4.44 m and the accuracy rate of only 70.4%. However, such a tracking error is neither receptable nor practical in usage.

Fig. 3 proves strongly practical meaning of NDO in control algorithm. Thus, one may lead to a conclusion that the designed NDO can not only estimate the disturbance in system, but also maintain the stability of system under serious SNR. Fig. 4 shows the flight trajectories of fixed-wing UAV under different sea conditions of level 7, 5, 4 with the significant sea waves height of

Table 5. Accuracies of tracking

$N_7 = 7.62$ m	$N_5 = 4.04$ m	$N_4 = 1.69$ m
98.52%	99.71%	99.30%

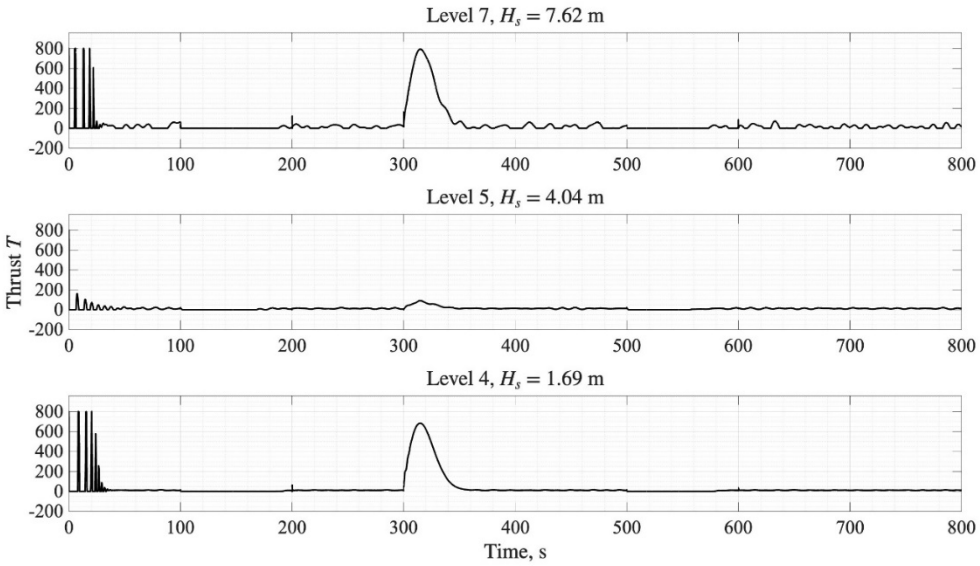

Figure 5. Thrust

7.62 m, 4.04 m, 1.69 m. The initial height of UAV is 50 m, after cruise stage the desired height is 15 m. It is not difficult to find out that designed Backstepping control algorithm maintains its stability under all sea conditions. Under condition of sea level 7 with wave height of 7.62 m, tracking error can be observed in the beginning of flight, two or three wave curves in the tracking trajectory indicate noticeable estimation error. The reason of them lies in 2 aspects: 1) it is impossible for one to pre-estimate the disturbance and give an appropriate value as the initial condition; 2) in the designing of control signal Eq. (21) we take into account $e_h, e_{2u}, \tilde{d}^2$, while during initial stage the tracking errors e_h, e_{2u} are relatively large. Seg. 1 in Fig. 4 shows details of this stage.

When it comes to severe sea condition (7.62m) on trajectories one can always observe small oscillations, which is showed in subfigure Seg. 3 in Fig. 4 in details. Considering that during such sea condition waves introduce into system large disturbance, the flight height is influenced in some ways. However, since the error in steady stage does not exceed 0.1m, the system still maintains its stability.

Sea condition of level 7 with the wave height of 7.62 m can be considered as one of the worst conditions during flight. We also checked the behaviour of system for sea condition of level 5 and 4. Since the flight condition and wave height are much better than level 7, tracking trajectories have better results. In Seg. 1 the orange, purple and red curves are trajectories of level 4, 5, 7, respectively, which indicates the relationship between sea condition and tracking error: the worse sea condition is, the larger tracking error becomes.

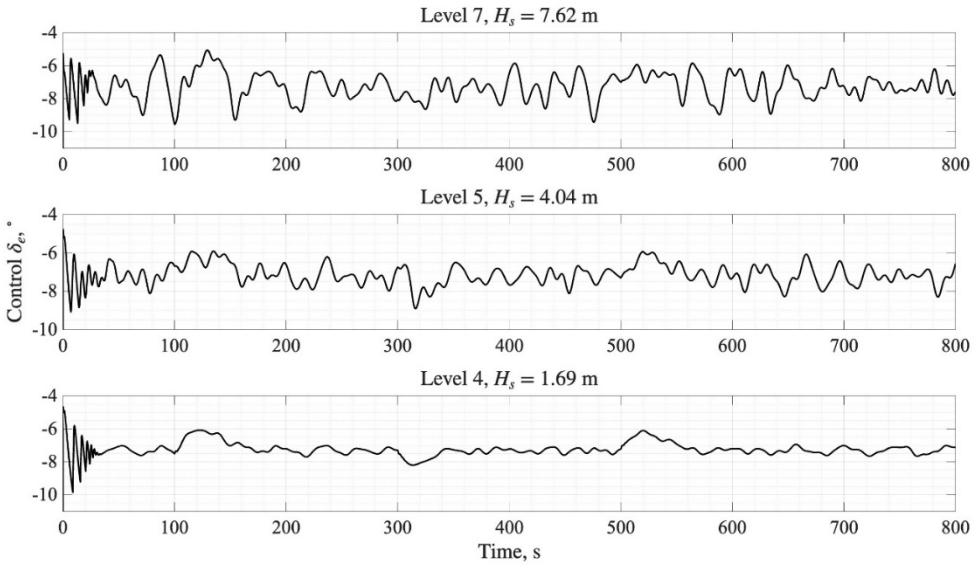

Figure 6. Elevator deflection

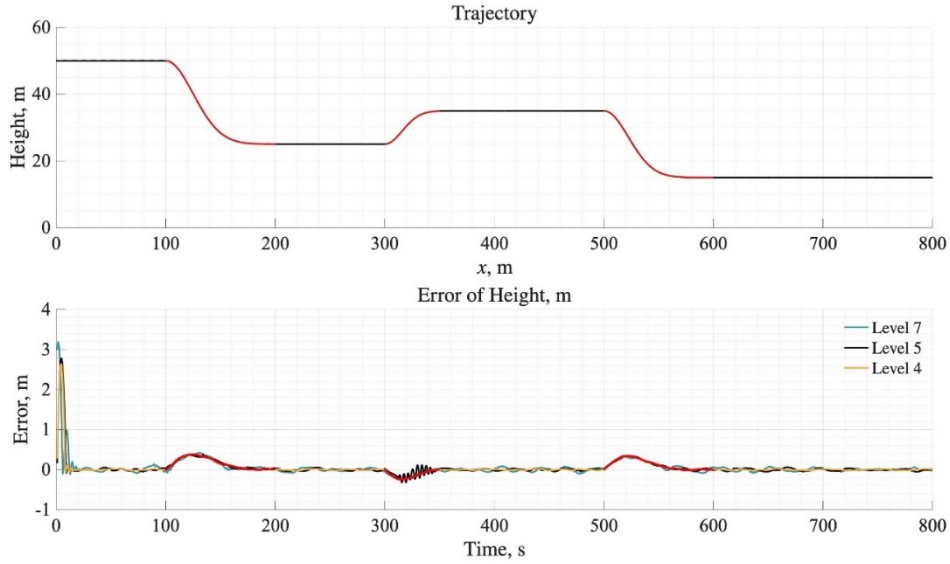

Figure 7. Error of height

If we claim the error area of ±3%, i.e. the difference between flight height and desired height shall not be larger than ±3%, then the accuracies of tracking can be listed as follows in Table 5.

Table 5 shows that the designed NDOAB method possesses a satisfying accuracy, even under one of the worst conditions it can still reach an accuracy of over 98%.

Table 6. Maximum errors and RMSE of level 7, 5, 4

Sea condition	$N_7 = 7.62$ m	$N_5 = 4.04$ m	$N_4 = 1.69$ m
Max. Error, m	3.1876	2.7838	2.6424
RMSE, m	0.2512	0.2269	0.2112

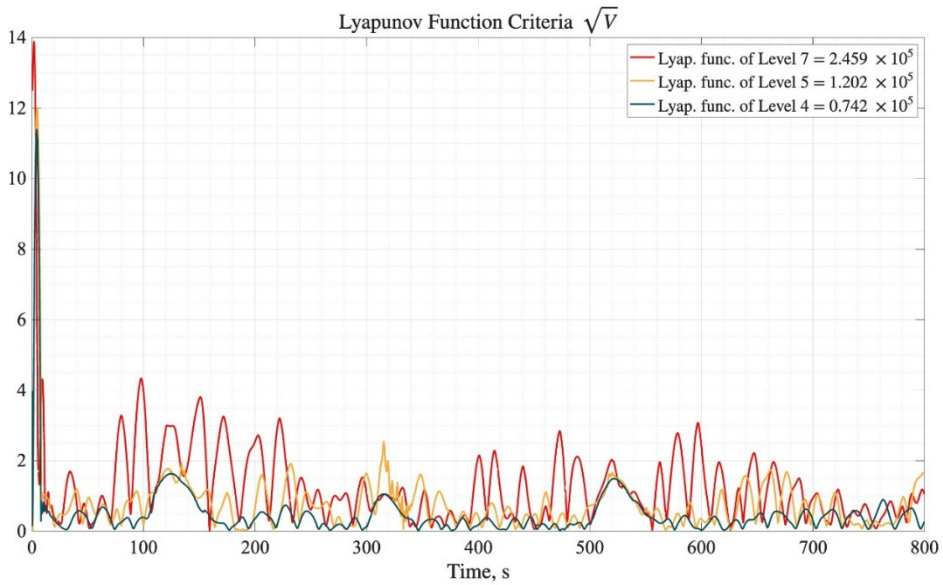

Figure 8. Lyapunov functions

Fig. 5 and Fig. 6 show control thrust and controlling elevator deflection, respectively. The thrust reaches its upper bound $\bar{T} = 800$ several times. It can be discovered that the change of upper bound of thrust approximately does not affect the behaviour of system. On the other hand, the changing range of δ_e doesn't over exceed its upper bound 30°, which indicates the safety of control.

Fig. 7 shows the error of flight height of level 7, 5, 4. It can be observed that the flight error decreases with the decrease of sea condition. The maximum error and RMSE (root mean squared error) of each sea condition are listed in Table 6. Other than that, during some fixed periods of time the error enlarges (we mark them in Fig. 7 with red colour). The same periods are marked in trajectory, and we can notice that such patterns occur when there are descent stage and climbing stage in trajectory. Apparently, they occur also, in other words, when UAV finish certain manoeuvres, posing to system serious disturbance.

Fig. 8 shows the Lyapunov function of sea condition level 7, 5, 4 according to Eq. (22). For the convenience of data showing in Fig. 8 we plot the root of Lyapunov function $\sqrt{V}$ other than its original value. As predicted in Eq. (24) Lyapunov function strive to zero with the error decreases to 0 ($e_h, e_{2u}, \tilde{d} \to 0$). Moreover, we calculated the integration of Lyapunov function, indicating that the integration decreases from 1.139×10^7 to 1.268×10^7 with the sea condition level.

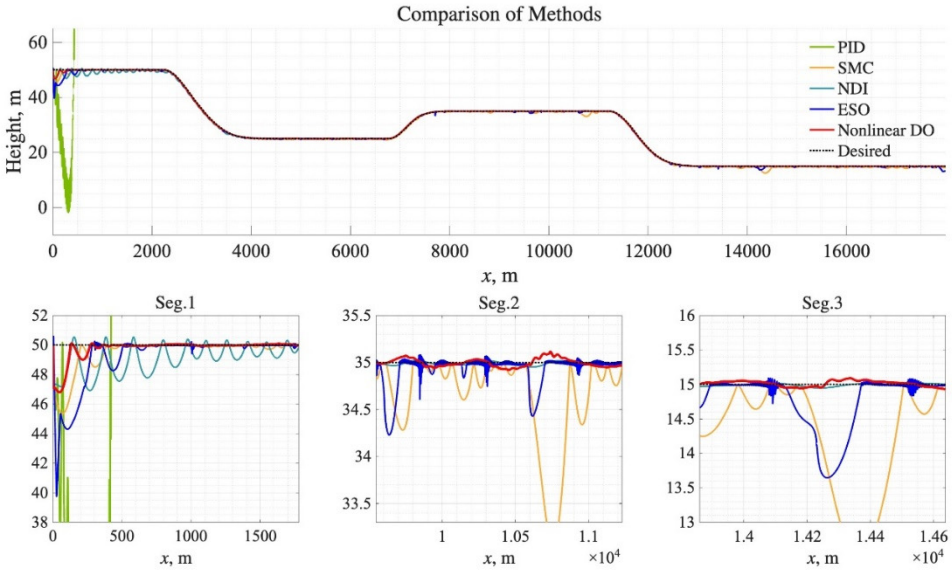

Figure 9. Comparison of different control methods

Fig. 9 is the comparison of different control methods – PID, SMC (sliding mode control), NDI (nonlinear dynamic inverse), ESO (extended state observer) with the proposed Backstepping method based on NDO (NDOAB). Here we list the following analysis:

(1) As a classical control method for linear systems, PID lost its stability in shorter than 500m (the first 2.82% distance of total flight), although it behaves strongly for linear systems. Turns out that when facing severe nonlinear and coupled systems such as fixed-wing UAV, PID cannot guarantee the system stability.

(2) SMC is well known as a robust control method against external disturbance. One may find in Seg. 2 and Seg. 3 in Fig. 9 that SMC has stronger oscillation along h-axis during flight, compared with proposed method, and even the shown behaviour from SMC is based on NDO also. One of the probable reasons of this phenomenon is: SMC during steady stage always demonstrates tiny but non-neglectable oscillation. Though the NDO can cancel the effect from sea wave to a certain extent, the estimation error $\tilde{d}$ enlarges the disturbance effect itself, which consequently enlarges the oscillation in SMC. From Seg. 2 one of the largest oscillations can reach 1.5m, which is not acceptable for a UAV.

(3) NDI is widely used nowadays, whereas it's high sensibility to disturbance requires suitable measures. In Seg. 2 and Seg. 3 it is shown that NDI can maintain the stability of steady cruise stage, while in Seg. 1 in initial stage NDI shows more oscillations with height error of 3m than proposed method. On the contrary the proposed Backstepping method based on NDO converges to desired height in 13s.

As another disturbance-resisting method, ESO serves to estimate the disturbance in system as an extended state. Generally it contains nonlinear coefficient function combined with sign function to compensate the effect of disturbance: $\dot{x}_1 = \hat{x}_2 + \beta_1 |e|^{0.5} \mathrm{sgn}(e)$. Some researchers [36] have proved that the coefficient β_1 may cause magnified gains on disturbance in signals, and is more suitable for ramp- or sinusoidal-like disturbance other than sea waves; moreover the sign function

Table 7. RMSE of different control methods

Method	RMSE, m	Method	RMSE, m
NDOAB	**0.2512**	SMC	0.4361
Backstepping	1.2626	NDI	0.4634
PID	25789 (failed)	ESO	0.6568

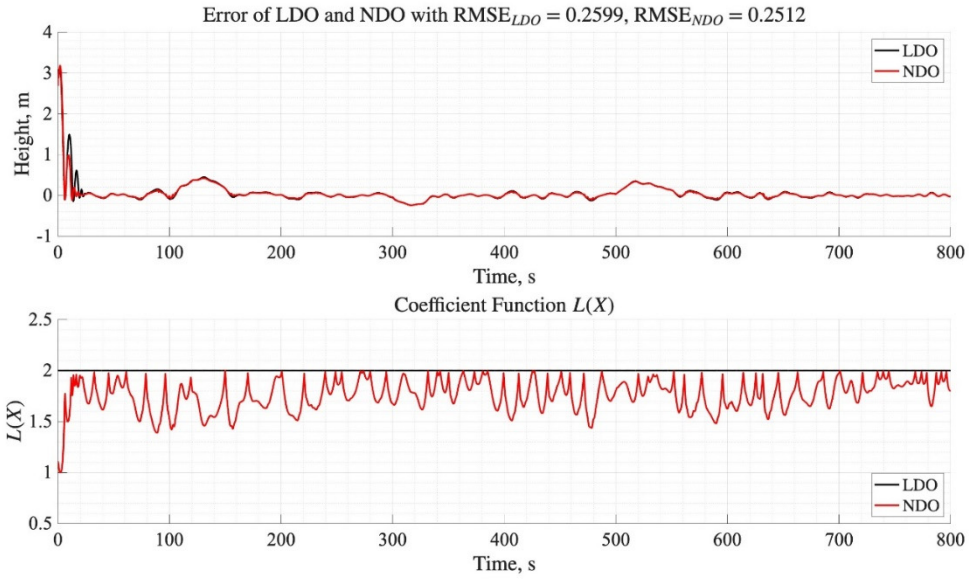

Figure 10. Comparison of LDO and NDO

shall also introduce into frequent switch of signal, which can be seen from Seg. 2 and Seg. 3. On the contrary, the proposed method can nonlinearly adapt to the disturbance according to Eq. (20), reducing the oscillations in system.

The RMSE of different control methods are shown in Table 7. Compared with widely used disturbance-resisting method, such as SMC and ESO, the proposed NDOAB can improve the performance for 42.40% and 61.75%.

We also compare the behaviour of linear disturbance observer (LDO) and NDO in Fig. 10. In LDO the coefficient function $L(\boldsymbol{X})$ is constant other than Eq. (20). It's obvious that the nonlinear $L(\boldsymbol{X})$ used in this paper will adjust itself during flight within the bound $L_0 = 2$, while the LDO of $L \equiv 2$ may cause the overshooting due to the large gain in LDO for some moments of time. On the other hand, the proposed $L(\boldsymbol{X})$ can stimulate the flight error e_h converge to zero with a higher rate and stronger stability, especially for the beginning 30s.

7. Conclusions

In this paper we proposed a reasonable mathematical model of sea-skimming fixed-wing UAV with consideration of external disturbance on system. The main component of external disturbance

is the height of sea waves. To improve the behavior of system under the effect of disturbance we designed a Backstepping control algorithm based on Lyapunov stability theory. In order to compensate the influence of disturbance we designed a nonlinear disturbance observer (NDO), which can estimate the disturbance with an adaptive nonlinear coefficient function. By assuming the existence of upper bound of disturbance we proved the stability of designed algorithm. Meanwhile the Lyapunov function in time domain is found to prove the rationality on the meaning of energy-saving. The simulated results Figs. 3-10 prove the stability and practicality of designed algorithm. It is shown in results that the designed NDOAB algorithm can guarantee stability of system under the sea condition of level 7 (significant wave height 7.62m); for better conditions system has better performances. The NDO can adjust the coefficient function based on the flight error information, bringing into system compensating information. Compared with other control methods, the proposed NDOAB method has satisfying behavior and smallest RMSE, showing its strong stability and high robustness. Some sharp fluctuations are still observed in the controlled trajectory, and future work will focus on estimation smoothing and prior data-processing.

Acknowledgments

This paper is funded by China Scholarship Council, project "2024 professional talent Training Program in Russia, Ukraine and Belarus", and was supported in part by the Russian Science Foundation under Grant 23-79-10028.

References

1. Lesieutre, D., Nixon, D., Torres, M.S.T. (1990). Analysis of missiles flying low over various sea states. Proceedings of the 17th Atmospheric flight mechanics conference, Portland, Oregon, August.
2. Aksu, T., Dülgar, Ö., Soken, H. (2024). Steep descent control algorithm for shipborne sea-skimming missiles. Proceedings of the 2024 CEAS EuroGNC conference, Bristol, UK, June.
3. Jing, Z., Cao, D., Meng, F., Li, J. (2024). Altitude control of UAV sea-skimming flight in ground effect area based on ADRC. Proceedings of the 7th International conference on computer information science and application technology (CISAT), Hangzhou, China. July.
4. Talole, S.E. and Phadke, S.B. (2002). Height control system for sea-skimming missile using predictive filter. Journal of Guidance Control and Dynamics, 25, 989-992. https://doi.org/10.2514/2.4977.
5. Dulgar, O., Gezer, R.B., Kutay, A.T. (2016). Extended kalman filter based robust altitude controller for sea skimming missiles. Proceedings of the AIAA Guidance, navigation, and control conference, San Diego, USA, January.
6. Li, J.S., Zhuang, L., Song, J.H., Chen, G., Hu, J. (2020). An altitude combined filter for suppressing various disturbances in sea skimming flight. Journal of Chinese Inertial Technology, 28, 522-527. https://doi.org/10.13695/j.cnki.12-1222/o3.2020.04.017.
7. Tan, Y.Y., Xu, A., Zhu, X.P., Zhou, Z. (2013). Optimizing and designed hybrid altimeter filtering system for small sea-skimming unmanned aerial vehicle (UAV). Journal of Northwestern Polytechnical University, 31, 511-516. https://doi.org/10.3969/j.issn.1000-2758.2013.04.002.
8. Xue, Y., Gu, W., He, P., Wu, G. (2010). Design of an adaptive stepping sliding mode controller for uncertain anti-ship missiles. Proceedings of the 3rd International conference on computer science and information technology, Chengdu, China, July.
9. He, P.C., Jia, L.S., Wang, Y.L., Zhang, W.G. (2012). Design of an adaptive terminal dynamic sliding mode controller for anti-ship missiles. Applied Mechanics and Materials, 187, 190-195.

https://doi.org/10.4028/www.scientific.net/AMM.187.190.
10. Dong, Q., Zong, Q., Tian, B., Wang, F. (2016). Adaptive-gain multivariable super-twisting sliding mode control for reentry RLV with torque perturbation. International Journal of Robust and Nonlinear Control, 27, 620-638. https://doi.org/10.1002/rnc.3589.
11. Zhao, H.C., Gu, W.J., Wang, R.Q. (2005). Adaptive global sliding mode variable structure control for anti-ship missile. Control Engineering of China, 12(4), 320-322. https://doi.org/10.3969/j.issn.1671-7848.2005.04.010.
12. Jiang, Z., Tang, X., Fan, X., Zhang, S. (2024). Height control of supersonic sea-skimming missiles based on online parameter identification. International Journal of Aerospace Engineering, 2024, 1-14. https://doi.org/10.1155/2024/1690034.
13. Wang, C., Ma, J.J., Zhang, X.L., Wang, X.G., Wu, X.F. (2023). Backstepping sliding mode control of hypersonic guided projectiles based on disturbance compensation. Journal of Gun Launch & Control, 44, 39-45. https://doi.org/10.19323/j.issn.1673-6524.2023.02.007.
14. Qin, H.Y., Chen, Z.Q., Sun, M.W., Zhou, Y., Sun, Q.L. (2023). Longitudinal control of nonlinear supercavitating vehicle based on extended state observer and backstepping method. Control Theory & Applications, 40, 373-380. https://doi.org/10.7641/CTA.2022.20085.
15. Zhou, Q.X., Wang, Y., Sun, X.A. (2022). Control of unmanned aerial vehicle based on gain adaptive super-twisting sliding mode theory. Journal of Shanghai Jiao Tong University, 56, 1453-1460. https://doi.org/10.16183/j.cnki.jsjtu.2022.238.
16. Zhou, Y.W., Zhong, K.W., Zhang, W.C., Jin, Y.H., Jiang, H.C. (2022). Adaptive attitude control of super-twisting sliding mode for near space vehicle. Aerospace Control and Application, 48, 9-15. https://doi.org/10.3969/j.issn.1674-1579.2022.01.002.
17. Liu, Y. (2021). Sea-skimming tracking control for high-speed aircrafts with great slenderness ratio. M.E. Dissertation, Shanghai University, Shanghai, China.
18. Priyamvada, K.S., Olikal, V., Talole, S.E., Phadke, S.B. (2011). Robust height control system design for sea-skimming missiles. Journal of Guidance, Control, and Dynamics, 34, 1746-1756. https://doi.org/10.2514/1.53577.
19. Yang, Z.G., Sun, P. (2021). Wave simulation based on combination of Gerstner function and Jonswap wave spectrum. Journal of Harbin University of Commerce (Natural Sciences Edition), 37, 676-682. https://doi.org/10.19492/j.cnki.1672-0946.2021.06.007.
20. Pan, C.P., Gu, W.J., Wang, G.Y., Liang, Y. (2006). The sea wave model establishment and verifying of anti-ship missile weapon system precision simulation. Journal of Projectiles, Rockets, Missiles and Guidance, 26, 546-549. https://doi.org/10.15892/j.cnki.djzdxb.2006.s7.015.
21. Guo, X.J., Cheng, X. (2010). Simulation of random sea wave model. Sichuan Binggong Xuebao, 31, 134-136. https://doi.org/10.3969/j.issn.1006-0707.2010.08.044.
22. Cai, F., Shi, A.G., Miao, Q.M. (2008). Bimodal wave model and its numerical simulation. Proceedings of ship safety management, Harbin, China, July.
23. Qi, N., Xia, T., Li, W.Y., Zhao, L.G. (2013). Simulation of the mathematical model of 3-D irregular wave based on MATLAB. Computer Knowledge and Technology, 9, 5737-5739.
24. Li, Y., Chen, X., Fei, S.M. (2014). The research on influence of wave of pneumatic performance of sea-skimming cruise missile. Journal of Projectiles, Rockets, Missiles and Guidance, 34, 129-132. https://doi.org/10.15892/j.cnki.djzdxb.2014.03.024.
25. Fossen, T.I. (1994). Guidance and control of ocean vehicles. John Wiley & Sons, Throndheim, Norway.
26. James, J.P., Panchang, V. (2022). Investigation of wave height distributions and characteristic wave periods in coastal environments. Journal of Geophysical Research: Oceans, 127, 1-21. https://doi.org/10.1029/2021JC018144.
27. Jia, C., Jin, C.J. (2022). New super-twisting sliding mode control strategy based on extended state observer. Control and Instruments in Chemical Industry, 49, 133-143. https://doi.org/10.3969/j.issn.1000-3932.2022.02.003.
28. Wu, K. (2019). Extended-state-observer-based disturbance rejection control for several classes of uncertain nonlinear systems. Ph.D. Dissertation, Southeast University, Nanjing, China.

29. Li, Y.T., Liu, X.D., Zhang, H.P., Wang, X.D. (2021). Attitude control method based on intelligent PID and extended state observer. Aerospace Control, 39, 51-58. https://doi.org/10.16804/j.cnki.issn1006-3242.2021.04.007.
30. Zeng, Z.Y., Li, Y.H. (2022). Research on flight control system of quadrotor UAV based on extended state observer. Small and Special Electrical Machines, 50(1), 41-44. https://doi.org/10.3969/j.issn.1004-7018.2022.01.009.
31. Ding, C. (2018). Nonlinear disturbance observer-based control for the trajectory tracking control of underactuated systems. M.E. Dissertation, Xiangtan University, Changsha, China.
32. Zhao, J., Wang, P., Sun, Y.F., Xu, F.Y., Xie, F. (2022). Nonsingular fast terminal sliding mode control based on nonlinear disturbance observer for a quadrotor. Transactions of Nanjing University of Aeronautics & Astronautics, 39, 219-230. https://doi.org/10.16356/j.1005-1120.2022.02.008.
33. Yue, Y.P. (2021). Research on trajectory tracking control for quadrotor based on disturbance rejection observer. M.E. Dissertation, Yanshan University, Qinhuangdao, China.
34. Xu, Z.Y., Cheng, Y., Wei, Y.F. (2022). Control for trajectory tracking of second order underactuated system based on nonlinear disturbance observer. Computer Applications and Software, 39, 88-92. https://doi.org/10.3969/j.issn.1000-386x.2022.08.013.
35. Li, J., Wan, L., Li, J., Hou, K. (2023). Adaptive backstepping control of quadrotor UAVs with output constraints and input saturation. Applied Sciences, 13, 1-17. https://doi.org/10.3390/app13158710.
36. Madoński, R., Herman, P. (2015). Survey on methods of increasing the efficiency of extended state disturbance observers. ISA Transactions, 56, 18-27. https://doi.org/10.1016/j.isatra.2014.11.008.